curve (Bordas *et al.*, 1977; Buras *et al.*, 1979) or by an expansion of a power function (Glazer *et al.*, 1978). Alternatively, it may be determined experimentally by the use of standards measured under the same conditions as the experiment (Scarlett *et al.*, 2009). This latter approach allows some separation of the contributions from the instrument and the sample, and allows some degrees of freedom in the refinement of sample-related parameters that may be of benefit in dynamic experiments. Other contributions to the diffraction pattern that must also be accounted for include any fluorescence peaks arising from the sample or shielding or collimators, and any detector escape peaks from both diffracted and fluorescence peaks. Fluorescence peak positions and relative intensities should be constant throughout the measurement and may therefore be modelled using a fixed 'peak group' whose overall intensity can be refined during analysis. Escape peaks can be accounted for by the inclusion of a second phase identical to the parent phase but with an independent scale factor and a constant energy offset determined by the nature of the detector (Rowles *et al.*, 2012).

Currently, few Rietveld software packages are capable of dealing directly with the differences between EDD and ADD, specifically (i) the variance of structure factors as a function of energy, (ii) the nonlinear distribution of intensity in the incident beam as a function of energy further modified by a nonlinear detector response, and (iii) the preferential absorption of lower-energy X-rays by the sample/air. *TOPAS* (Bruker AXS, 2013) embodies algorithms that allow the pattern to be modelled directly on the energy scale and also the inclusion of equations to account for intensity variations arising from the experimental conditions. This allows quantification from such data to be achieved directly using Rietveld-based crystal-structure modelling incorporating the Hill and Howard algorithm in equation (3.9.26) (Hill & Howard, 1987). The application of *TOPAS* to a complex EDD experiment investigating the changes to the anode during molten-salt electrochemistry conducted in molten $CaCl_2$ at about 1223 K has been described by Rowles *et al.* (2012) and Styles *et al.* (2012).

### 3.9.10. Improving accuracy

There are many factors that influence the accuracy and precision of QPA results where (i) accuracy is defined as the agreement between the analytical result and the true value, and (ii) precision is the agreement between results if the analysis is repeated under the same conditions. Precision may further be split into (i) repeatability, which is the agreement between repeated measurement and analysis of the same specimen, and (ii) reproducibility, which additionally includes re-preparation, measurement and analysis of the sample.

#### 3.9.10.1. *Standard deviations and error estimates*

Determination of the actual accuracy of an analysis is not a trivial task in a standardless method. In fact, it cannot be achieved without recourse to another measure of the sample that does incorporate standards. Too often, analysts will report Rietveld errors calculated in the course of refinement as the errors in the final quantification. However, these numbers relate purely to the mathematical fit of the model and have no bearing on the accuracy of the quantification itself.

Consider, for example, a three-phase mixture of corundum, magnetite and zircon. Such a sample was presented as sample 4 in the IUCr CPD round robin on QPA (Scarlett *et al.*, 2002). Its components were chosen with the deliberate aim of creating a sample in which severe sample-related aberrations occur. Table 3.9.4 shows the weighed amounts of each component and the results of replicate analyses of three different sub-samples of this material.

**Table 3.9.4**
Comparison of errors generated during the analysis of XRD data (Cu $K\alpha$ radiation) from three sub-samples of sample 4 from the IUCr CPD round robin on QPA (Scarlett *et al.*, 2002)

The bias values are (measured − weighed) while the values denoted XRF are the phase abundances generated from elemental concentrations measured by X-ray fluorescence methods.

| | Phase | | |
|---|---|---|---|
| $n$ = 3 | Corundum | Magnetite | Zircon |
| Weighed | 50.46 | 19.46 | 29.90 |
| Mean XRD measured wt% | 56.52 | 17.06 | 26.42 |
| Mean of Rietveld errors | 0.15 | 0.11 | 0.11 |
| Standard deviation of measured wt% | 0.63 | 0.41 | 0.35 |
| Mean of bias | 6.06 | −2.58 | −3.48 |
| XRF | 50.4(2) | 19.6(1) | 29.5(1) |

It is apparent that the standard deviation of the mean abundances of the three replicates, which represents the expected precision in the analysis, is 3 to 4 times greater than the errors reported by the Rietveld software. The good level of fit achieved in conducting these analyses (evidenced by low $R$ factors) could lead the analyst to conclude that the mean value ± the standard deviation of the mean is an adequate measure of the phase abundances and their errors.

However, both the Rietveld errors and the precision are at least an order of magnitude smaller than the bias. The large bias, in this case due to the presence of severe microabsorption, represents the true accuracy that can be achieved in this example. Unfortunately, there is nothing in the XRD data and Rietveld analysis process that indicates that there may be a problem. It is only when the QPA is compared with other estimates, in this case derived from XRF chemical-analysis results, that the problem becomes apparent. The analyst must take further steps to identify sample-preparation and/or data-collection protocols that may improve accuracy and, importantly, seek ways to verify the results.

#### 3.9.10.2. *Minimizing systematic errors*

The fundamental measured quantities in a diffraction pattern are the integrated intensities of the observed peaks. The precision of these measurements can be improved by: (i) increasing the primary intensity of the diffractometer using optics or higher-power X-ray sources; (ii) using scanning linear detectors (see Chapter 2.1), which have multiple detector elements to collect individual intensities many times; these are then summed to achieve higher accumulated counts; (iii) increasing the number of counts accumulated at each step, that is increasing the step counting time $T$; and (iv) increasing the number of points, $N$, measured across the peak.

Often, the temptation is to collect data with large values of $N$ and $T$ to maximize counting statistics. However, the resulting increased precision is only useful up to the point where counting variance becomes negligible in relation to other sources of error; thereafter data-collection time is wasted. For example, if the sample is affected by the presence of severe sample-related

aberrations, the collection of highly precise data will not improve the accuracy of the resulting analysis significantly.

Therefore, the most important approach to improving the accuracy of an analysis is to eliminate the systematic errors. Given that the largest sources of error in QPA are experimental (Chung & Smith, 2000) and relate to sampling and specimen preparation, then this is the area on which the most careful attention needs to be focused. A detailed discussion of sample preparation and data-collection procedures is beyond the scope of this chapter but further details can be found in Chapter 2.10, and in Hill & Madsen (2002) and Buhrke *et al.* (1998).

#### 3.9.10.3. *Minimizing sample-related errors*

##### 3.9.10.3.1. *Crystallite-size issues*

Crystallite size is considered here as the length of a coherent scattering domain and should not be confused with the terms grain or particle size used frequently in powder diffraction to describe the macroscopic size of the components in the sample. The macroscopic size of the particle is somewhat irrelevant (as in ceramics or other solid pieces of samples) as long as the crystallites (or domains) that comprise the particle are (i) sufficiently small to ensure that there are enough crystallites contributing to the diffraction process (Smith, 1992) and (ii) randomly oriented, thus ensuring a true powder-average representation of intensities. However, for large domains or crystallites this assumption is usually not fulfilled and therefore it is necessary to reduce the crystallite size by reducing the size of the particles or grains that constitute the macroscopic objects of a powder.

Most issues in sample preparation are related to crystallite size and preferred orientation of the particles in the sample holder. For QPA a representative sampling of all possible orientations of crystallites with respect to the diffraction geometry is required. Rotation of the sample improves the particle statistics, since more crystallites can satisfy the diffraction condition (Elton & Salt, 1996).

Large-crystallite issues are easily detected using two-dimensional (2D) detectors, where the Debye rings show a 'spotty' intensity distribution. However, most QPA measurements are performed using 0D (point) or 1D (strip) detectors. The effect of large crystallites in a 1D pattern is that a few crystallites may contribute to irregularly high intensities for selected reflections. In the diffraction pattern, this situation is usually identified by intense reflections having a sharp peak profile compared with the surrounding peaks in the pattern. Furthermore, in a Rietveld refinement this situation is manifested by large intensity differences between the observed and calculated pattern that may not be associated with a particular crystallographic direction and hence to preferred orientation. Another way of detecting inhomogeneous crystallite distributions is to measure a series of scans from the same specimen at various rotation angles and comparing the relative peak intensities. It is worth noting that the push towards ever higher resolution in both laboratory and synchrotron instruments serves to further exacerbate the crystallite-size issue. This arises from the use of beams with decreased divergence, resulting in fewer crystallites likely to satisfy the diffraction condition.

There is no simple mathematical correction for large-crystallite issues and the effect is often misinterpreted in Rietveld refinement as preferred orientation. In this case, the correction would typically involve use of several directions for March–Dollase-type functions (Dollase, 1986) or an increasing order of spherical-harmonics coefficients (Ahtee *et al.*, 1989). In any case, this is an improper use of these corrections and the necessity to do so clearly points to deficiencies in the sample preparation and data-collection regime.

The best way to minimize the large-crystallite issue is to reduce the crystallite size through grinding of the sample. However, size-reduction methods need to be carefully assessed, since over-grinding can cause peak broadening due to (i) a decrease of long-range order and hence crystallite size and (ii) the introduction of microstrain (Hill & Madsen, 2002). The practical effect of peak broadening is increasing peak overlap, which may complicate the phase identification. For whole-pattern-based QPA, overgrinding is not as serious as long as it does not yield nanometre-sized particles or amorphous materials. This is because the integral intensity of the peaks is preserved. It should be noted that some phases can undergo transformation to other polymorphs or decompose to other phases during grinding (Hill & Madsen, 2002).

In practice, there is no generally applicable comminution strategy. For each material, a suitable milling device and grinding strategy needs to be identified. Inhomogeneous materials such as ores, concentrates and other mineralogical materials may have very different comminution properties for their constituents, leading to size fractionation during grinding. Large-crystallite issues are frequently observed for hard minerals (*e.g.* quartz, feldspar) while the grain size of soft minerals (*e.g.* talc) is reduced more rapidly.

A practical way of finding a best compromise for the milling conditions of a mixture may be the analysis of a series of samples of the same material where, for example, the grinding time is successively increased and the quantification results are compared. Fig. 3.9.17 shows the variation of analysed wt% with grinding time for two minerals: a stable result is eventually obtained.

There is a more extensive discussion of the impact of large-crystallite size on observed diffraction data (Smith, 1992) and ways to minimize its effect (Elton & Salt, 1996) in the published literature.

##### 3.9.10.3.2. *Preferred orientation*

In order to generate peak intensities that accurately represent the intensity-weighted reciprocal lattice, the crystallites in the powder must not only be sufficient in number, but they must also be randomly oriented. In other words, each crystal orientation should have the same probability of diffracting. Preferred orientation can arise when particles align in the sample holder according to their morphology. This is most common with platy or

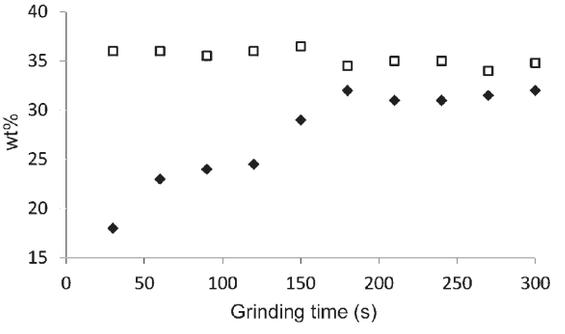


**Figure 3.9.17**
Variation of the magnetite (filled diamonds) and quartz (open squares) concentration of an iron-ore sample with grinding time. Stable conditions are obtained after about 180 s. Data courtesy ThyssenKrupp – Resource Technologies (Knorr & Bornefeld, 2013).

needle-like materials and the effect on the diffraction pattern is the observation of enhanced intensity along specific crystallographic directions with a subsequent decrease of intensity along other directions.

A number of sample-presentation methods can be used to minimize preferred orientation. For flat specimens, back pressing and side drifting into the sample holder can be effective. These methods tend to produce much less preferred orientation than front-mounted samples, but tend not to be very effective for chronic preferred orientation such as that exhibited by phases like clays, feldspars and chlorite. Reducing the size of the crystallites improves the probability of achieving random alignment of the crystallites in the sample holder. Gradually milling a sample and monitoring the preferred-orientation coefficients as a function of grinding time may again help to find the correct, or at least reproducible, grinding conditions (Fig. 3.9.18).

A major advantage of whole-pattern-based QPA over single-peak methods is that all classes of reflections are considered in the calculation. In this sense, the method is less prone to preferred orientation of a particular class of peaks. Furthermore, orientation effects may be corrected by applying March–Dollase (Dollase, 1986) or spherical-harmonics (Ahtee *et al.*, 1989) corrections. A properly applied correction may be of high importance for QPA in cases where a phase is present at low concentration and only a few peaks can clearly be identified in the pattern. If those peak(s) are affected by preferred orientation, the March–Dollase coefficient correlates strongly with scale factors and leads to biased QPA results. Examples of this effect occur with layered materials that have sheet-like morphology perpendicular to the *c* axis, including mica and clay minerals, which typically show stronger than expected intensity for the 00*l* reflections.

The crucial factor seems to be to what extent the orientation parameters correlate with the Rietveld scale factor. An example where the correlation is only minor is sample 2 from the IUCr CPD round robin on QPA (Scarlett *et al.*, 2002). In that example, brucite [$Mg(OH)_2$] shows strong preferred orientation along the 00*l* direction. This may be corrected by the March–Dollase model, which returns a refined value of 0.66. However, the introduction of this preferred-orientation correction only changes the brucite concentration from 35 to 36 wt% (weighed = 36.36 wt%); this is surprising because the orientation is strong and the weighted residual $R_{wp}$ changes from 30 to 15%. Close examination of the correlations reveals a strong correlation between the brucite scale factor and preferred-orientation factor.

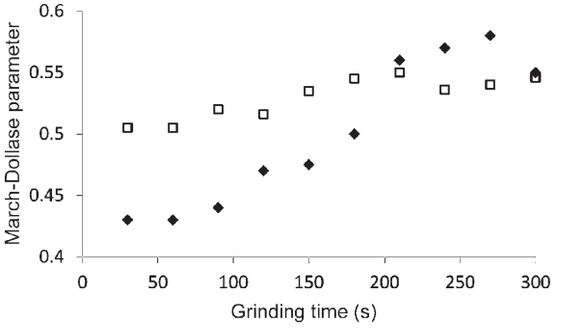


**Figure 3.9.18**
Increase of the March–Dollase (Dollase, 1986) parameter and related decrease of the degree of preferred orientation with grinding time for the two amphibole species actinolite (filled diamonds) and grunerite (open squares) in an iron ore. Data courtesy ThyssenKrupp – Resource Technologies (Knorr & Bornefeld, 2013).

However, the correlation of the brucite preferred-orientation parameter to the other scale factors (zincite, corundum and fluorite) is close to zero; this explains why in this example the QPA is not highly dependent on preferred orientation. In cases of strong correlation between the orientation parameter of one phase and the scale factors of other phases, preferred orientation should probably not be refined, or at least it should be verified carefully. It is worth noting that, in all Rietveld-based analyses, users should examine the correlation matrix as a matter of general practice to establish which parameters might be affecting parameters of interest.

It should be noted that sample rotation around the scattering vector (typically employed in flat-plate Bragg–Brentano geometry) during the scan does not reduce preferred orientation, since there is no change between the preferred-orientation direction and the diffraction vector. Using capillaries in transmission geometry assists in the reduction of preferred orientation, but the time-consuming nature of packing capillaries makes this technique infeasible in industrial applications where diffraction-based QPA is used for routine quality control.

#### 3.9.10.3.3. *Microabsorption*

The strongest on-going impediment to accuracy in QPA using XRD data is microabsorption. The microabsorption effect occurs when a multiphase sample contains both low- and highly absorbing phases. For the highly absorbing phases, the X-ray beam is more likely to be absorbed in the surface layers of the grain; thus, the fraction of the grain contributing to the diffraction pattern will decrease as the size of the grain increases above the beam-penetration depth. For the low-absorbing phases, the beam penetrates further into the particle resulting in a greater likelihood of the desired 'volume diffraction' occurring (Brindley, 1945). The overall effect is the observation of a disproportionate amount of observed intensity from individual grains relative to what would be expected for the average absorption of the sample; the highly absorbing phases are under-represented relative to the low-absorbing phases. There is extensive discussion of the microabsorption issue in Zevin & Kimmel (1995).

Brindley (1945) has described the particle absorption contrast factor $\tau_\alpha$ as

$$\tau_\alpha = (1/V)\int_0^V \exp\left(-(\mu_\alpha - \bar{\mu})\right) \mathrm{d}v, \qquad (3.9.48)$$

where $V$ is the particle volume, and $\mu_\alpha$ and $\bar{\mu}$ are the linear absorption coefficients of phase $\alpha$ and the entire sample, respectively. While it is relatively easy to calculate the absorption coefficients, equation (3.9.48) implies knowledge of the *particle* size of each component; this information is only available through independent microscope or light-scattering characterization.

This correction term is commonly incorporated into QPA through a modification to equation (3.9.26) of the form

$$W_\alpha = \frac{S_\alpha (ZMV)_\alpha / \tau_\alpha}{\sum_{k=1}^{n} S_k (ZMV)_k / \tau_k}. \qquad (3.9.49)$$

Brindley has also devised criteria by which to assess whether a microabsorption problem is likely to be present or not. Calculation of $\mu D$ (where $\mu$ is the linear absorption coefficient and $D$ is the particle diameter) yields the following criteria:

(i) $\mu D < 0.01$ – fine powder. There is negligible microabsorption and hence no correction is necessary.

**Table 3.9.5**
Calculated values of $\mu D$ (where $\mu$ is the linear absorption coefficient and $D$ is the particle diameter) for Cu $K\alpha$ X-rays for corundum, magnetite and zircon with a range of particle sizes

| | $\mu D$ | | |
|---|---|---|---|
| Diameter (μm) | Corundum, $Al_2O_3$ ($\mu$ = 125 $cm^{-1}$) | Magnetite, $Fe_3O_4$ ($\mu$ = 1167 $cm^{-1}$) | Zircon, $ZrSiO_4$ ($\mu$ = 380 $cm^{-1}$) |
| 0.1 | 0.001 | 0.012 | 0.004 |
| 0.2 | 0.003 | 0.023 | 0.008 |
| 0.5 | 0.006 | 0.058 | 0.019 |
| 1 | 0.013 | 0.117 | 0.038 |
| 2 | 0.025 | 0.233 | 0.076 |
| 5 | 0.063 | 0.584 | 0.190 |
| 10 | 0.125 | 1.167 | 0.380 |
| 20 | 0.251 | 2.334 | 0.759 |

(ii) $0.01 < \mu D < 0.1$ – medium powder. Microabsorption is likely to be present and the normal Brindley correction model can be applied.

(iii) $0.1 < \mu D < 1.0$ – coarse powder. A large microabsorption effect is present. The Brindley model can only be used to provide an approximate correction provided that $\mu D$ is closer to the lower limit of the range.

(iv) $\mu D > 1.0$ – very coarse powder. This indicates that severe microabsorption is likely to be present and that any correction is well beyond the limits of the model.

It is difficult for the analyst encountering a new sample to determine whether a correction for microabsorption is required without first obtaining additional information. A minimum requirement should be to calculate $\mu D$ for each phase present. However, this requires knowledge of the particle size which, in a multiphase sample, can be very difficult to obtain unambiguously. Even when the particle size is measured by, for example, dynamic light scattering or optical or SEM image analysis, the applicability of the correction can still be unclear. In addition, the correction factor embodied in equations (3.9.48) and (3.9.49) makes the assumption that the particles of the phase of interest are spherical and of uniform size. This assumption is unrealistic in almost all samples; in reality, each phase is likely to be present at a wide range of particle sizes and the particles are highly unlikely to be spherical.

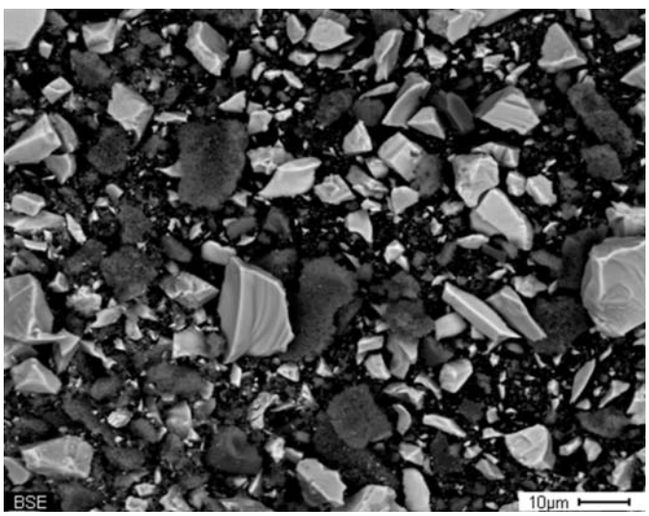


**Figure 3.9.19**
Backscattered-electron SEM image of a mixture of approximately equal amounts of corundum (dark grey), magnetite and zircon (lighter grey). Note the wide range of particle sizes present for each of the three phases.

Table 3.9.5 shows the calculated values of $\mu D$ for Cu $K\alpha$ radiation for some commonly encountered phases in mineralogical analysis. For the least absorbing phase (corundum), the upper range of applicability of the Brindley model (medium powder) is reached at about 5 μm; by 8 μm, the coarse powder criterion has been reached and the correction model is no longer applicable. For magnetite, these limits are reached an order of magnitude earlier at about 0.5 and 0.9 μm, respectively.

Fig. 3.9.19 shows an SEM image of a mixture of approximately equal amounts of corundum, magnetite and zircon. The individual components of the sample were weighed and the mixture ground in ethanol in a McCrone micronizing mill (McCrone Research Associates, London) for 10 min $g^{-1}$. This approach to sample preparation is generally accepted as best practice for powder XRD because it minimizes structural damage during grinding (Hill & Madsen, 2002). After decanting and drying, the sample was back-packed into a cavity sample holder for XRD data collection; the same sample was then used to obtain the SEM image in Fig. 3.9.19. Visual observation shows a wide range of particle sizes (from submicron to greater than 10 μm) and shapes that do not even approximate spheres. Even if this information is obtained, selection of a particle size that best represents each individual phase is a difficult task. In addition, in many sample suites, the component phases exhibit a range of hardness resulting in different rates of grinding and hence difference size ranges. Regrettably, what happens too often in practice is that analysts will micronize the sample and then select an arbitrary particle size in order to derive a 'preferred' value for the final analysis. Therefore, caution is advised in the application of these correction models. The IUCr CPD round robin on QPA (Madsen *et al.*, 2001; Scarlett *et al.*, 2002) showed that many participants severely degraded their results by applying a correction when none was necessary.

Equation (3.9.48) shows that there two ways to minimize microabsorption. The first is to reduce the absorption contrast by, for example, changing the X-ray wavelength. While corundum and magnetite have very different linear absorption coefficients for Cu $K\alpha$ radiation (126 and 1123 $cm^{-1}$, respectively), the difference is reduced to 196 and 231 $cm^{-1}$, respectively, for Co $K\alpha$ radiation. The second approach is to reduce the particle size in order to meet Brindley's fine- or medium-powder criteria.

However, even these steps may not be sufficient to eliminate the microabsorption effect. Slightly different absorption coefficients, or different particle sizes for phases with the same absorption coefficients, may still introduce a bias between expected and analysed concentrations. In this situation, it may be better to use a calibrated hkl_phase or peaks_phase (Section 3.9.6) instead of a Rietveld, structure-based phase. The calibration step involved in the generation of such a phase incorporates the microabsorption problem into the calibration constant.

Fig. 3.9.20 shows the bias between known concentrations (derived from chemical analysis) and QPA-determined concentrations for a series of salt samples. The samples contain halite (NaCl), sylvite (KCl) and kieserite ($MgSO_4{\cdot}H_2O$) as major phases and small amounts of anhydrite ($CaSO_4$), langbeinite [$K_2Mg_2(SO_4)_3$] and carnallite [$KMgCl_3{\cdot}6(H_2O)$]. The linear absorption coefficient of sylvite (254 $cm^{-1}$) is much higher than halite (165 $cm^{-1}$). Using crystal-structure-based analysis, there is a systematic deviation of up to 3% with an overestimation of the low absorber (halite) and an underestimation of the high absorber (sylvite). After replacing sylvite by a calibrated

hkl_phase, the bias is reduced to about 1% and does not show systematic deviations.

It should be noted, however, that the phase constants developed using such a calibration approach will only be applicable to the sample suite and preparation conditions for which it was developed. The calibration process will need to be repeated if there are significant changes to the sample suite or sample-preparation conditions.

3.9.10.3.4. *Whole-pattern-refinement effects*

One of the distinct advantages of structure-based whole-pattern fitting for QPA is that no standards need to be prepared because the structure for each phase provides the phase constant *ZMV*; the unit-cell dimensions allow the calculation of the cell volume *V* and the unit-cell contents provide the mass *ZM* (Bish & Howard, 1988; Hill & Howard, 1987). These values are used, along with the Rietveld scale factor *S*, in equation (3.9.26) to derive the phase abundance. This is especially useful for complex systems where the preparation of multiple standards would add considerably to the analytical complexity.

An additional advantage is the ability to refine the crystal structure (unit-cell dimensions and site-occupation factors, for example), when the data are of sufficiently high quality, in order to obtain the best fit between observed and calculated patterns. In addition to updating the *ZMV* value, the site occupancies are contained in the structure-factor calculation and, therefore, will change the relative reflection intensities and have an impact on the scale factor and QPA. Other structural parameters that have a strong effect on the scale factor and QPA are the atomic displacement parameters (ADPs). Strong correlation between the ADPs and amorphous material concentration has been shown by Gualtieri (2000) and Madsen *et al.* (2011).

This leads to the question: which crystal structure should be selected for QPA? Databases contain multiple entries for the same phase with the structures determined using different methods. While ADPs and site-occupation factors determined using neutron diffraction and single-crystal analysis should be favoured over those determined using X-ray powder data, many database entries do not have refined ADPs for all (and in some cases, any) atoms. Often, arbitrarily chosen default values of 0.5 or 1.0 $Å^2$ for $B_{eq}$ are entered for all atoms, but this should be viewed or used with great caution. There is clearly a need to carefully evaluate the crystal-structure data used for QPA. This is particularly worth mentioning in view of the advent of new 'user-friendly' software that automatically assigns crystal structures after having performed the phase identification.

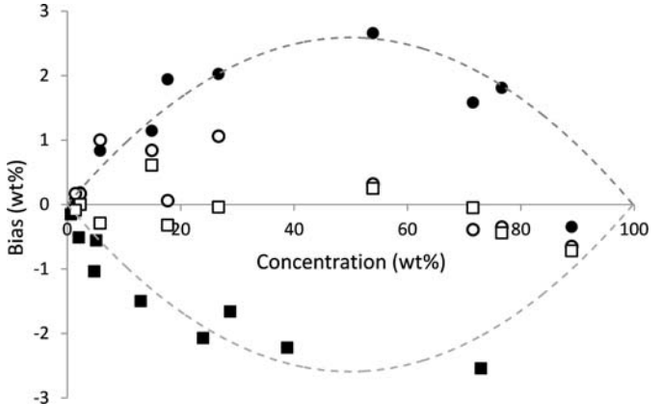


**Figure 3.9.20**
Bias as a function of phase concentration for industrial salt samples for (i) structure-based QPA (filled symbols) and (ii) calibrated hkl_phase (open symbols) for halite (circles) and sylvite (squares). The broken lines indicate the trend of the bias for structure-based QPA. Data are courtesy of K+S AG, Germany.

Empirical profile-shape models contribute significantly to the complexity (and correlations) of whole-powder-pattern fitting for QPA because of the large number of phases and multiple parameters required to model the profile shape of each phase. The use of convolution-based profile fitting [in, for example, *BGMN* (Bergmann *et al.*, 1998, 2000) and *TOPAS* (Bruker AXS, 2013)] greatly reduces the number of parameters, because the instrument-resolution function (which is constant for a given setup) can be separated from sample-related peak broadening. The instrument component can be refined using a standard and then fixed for subsequent analysis. The sample contribution to peak width and shape can then be related directly to crystallite size and microstrain using a minimal number of parameters. The reduction of the total number of parameters reduces the refinement complexity and the chance of parameter correlation.

The choice of the function used to model the pattern background may also have a strong influence on amorphous content (Gualtieri, 2000; Madsen *et al.*, 2011). Given that the intensities of both the background and the amorphous contribution vary slowly as a function of $2\theta$, it is inevitable that there will be a high degree of correlation between them. Hence, any errors in determining the true background will result in errors in amorphous phase determination. A simple approach is to use a background function with a minimal number of parameters. A more exact approach requires the separation of the amorphous contribution from background components such as Compton scattering and parasitic scattering by the sample environment and air in the beam path. This is routinely done in pair distribution function (PDF) analysis; details can be found in Chapter 5.7 in this volume and in Egami & Billinge (2003).

Another parameter that correlates with the pattern background is the width of broad peaks for phases of low concentration. If allowed to refine to very large width values, the peaks are 'smeared' over a broad range of the pattern with no clear distinction between peaks and background. The same issue applies when there is a high degree of peak overlap, particularly at high angles, leading to severe under- or over-estimation of the phase. The careful use of limits for either crystallite size or corresponding parameters in empirical peak-shape modelling assists in minimizing this effect.

There can be a subtle interplay between the profile-shape function and the pattern background that has an impact on whole-pattern fitting (Hill, 1992). The data in Fig. 3.9.21, collected using a Cu tube and an Ni $K\beta$ filter, exhibit low-angle truncation of the peak tails at the $\beta$-filter absorption edge. On the high-angle side, the anatase peak displays a wide tail which extends to the position of the strongest rutile peak at about 27.5° $2\theta$. In this case, rutile is present as a minor phase and the error in the background determination using conventional peak-profile modelling (Fig. 3.9.21*a*) introduces about 0.5% bias in the rutile QPA. The use of a more accurate profile model that incorporates the effect of the $\beta$-filter absorption edge (Fig. 3.9.21*b*) serves to improve the accuracy (Bruker AXS, 2013).

3.9.10.3.5. *Element analytical standards*

XRD-based derivation of elemental abundances relies on (i) the QPA abundances, and (ii) the assumed or measured stoichiometry of the crystalline phases. The accuracy of the QPA

**Table 3.9.6**
Compositional analysis of the Dillinger Hütte iron-ore certified reference material SX 11-14, (i) derived from QPA results, taking into account the nominal stoichiometry of the phases (XRD) and (ii) the certified analyses (Cert) (Knorr & Bornefeld, 2013)

| Phase | wt% | | Fe | FeO | $SiO_2$ | $Al_2O_3$ | MgO | CaO | $K_2O$ | $Na_2O$ | C |
|---|---|---|---|---|---|---|---|---|---|---|---|
| Haematite | 0.37 | | 0.26 | — | — | — | — | — | — | — | — |
| Goethite | 3.86 | | 2.43 | — | — | — | — | — | — | — | — |
| Magnetite | 85.97 | | 62.21 | 26.68 | — | — | — | — | — | — | — |
| Quartz | 5.73 | | — | — | 5.73 | — | — | — | — | — | — |
| Gibbsite | 0.71 | | — | — | — | 0.46 | — | — | — | — | — |
| Talc | 1.79 | | — | — | 1.13 | — | 0.57 | — | — | — | — |
| Orthoclase | 0.30 | | — | — | 0.19 | 0.05 | — | — | 0.05 | — | — |
| Albite | 0.89 | | — | — | 0.60 | 0.18 | — | — | — | 0.10 | — |
| Calcite | 0.40 | | — | — | — | — | — | 0.22 | — | — | 0.19 |
| | | | Fe | FeO | $SiO_2$ | $Al_2O_3$ | MgO | CaO | $K_2O$ | $Na_2O$ | C |
| | | XRD | 64.89 | 26.68 | 7.66 | 0.70 | 0.57 | 0.22 | 0.05 | 0.10 | 0.19 |
| | | Cert | 65.55 | 27.20 | 7.47 | 0.27 | 0.56 | 0.42 | 0.06 | 0.08 | 0.12 |
| | | Bias | −0.66 | −0.52 | 0.19 | 0.43 | 0.01 | −0.20 | −0.01 | 0.02 | 0.07 |

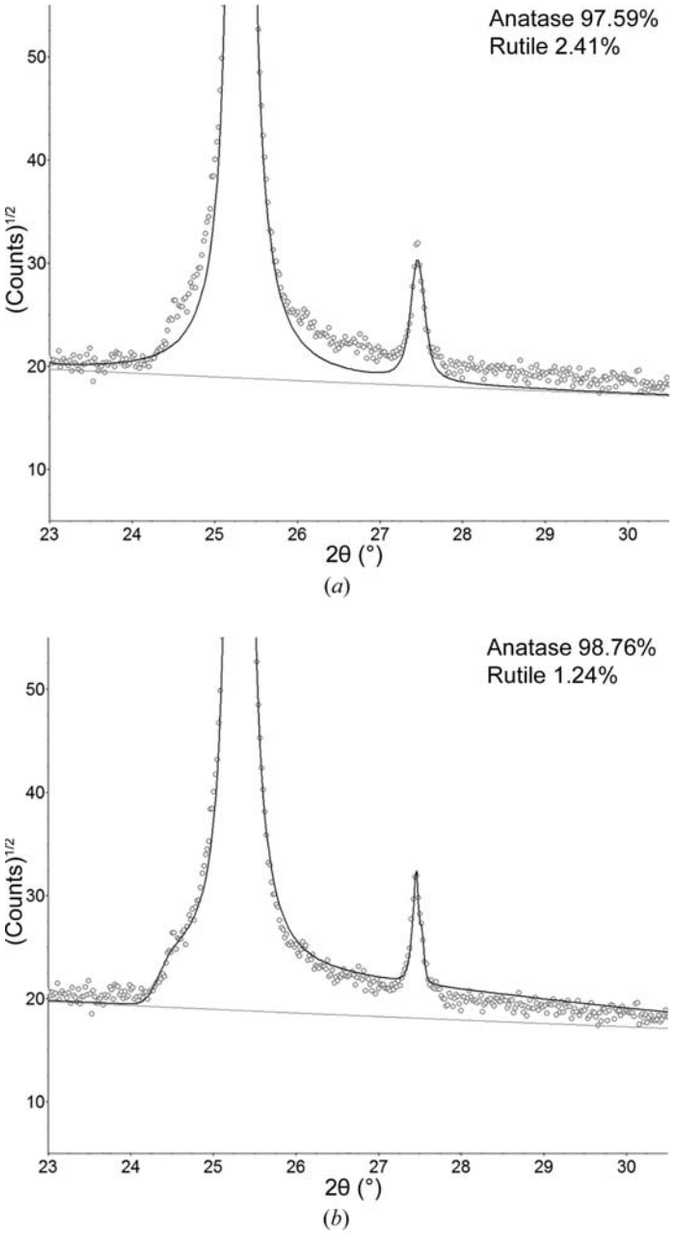


**Figure 3.9.21**
Profile fit of anatase and rutile (*a*) without and (*b*) with a $K\beta$ filter absorption-edge correction.

result may then be evaluated by comparing the calculated elemental abundances with those determined by traditional chemical-analysis techniques. However, for the best level of agreement, this method requires that the composition of the crystalline phases be well defined. A complication, in particular for minerals, is that idealized compositions may be reported but do not necessarily match the actual composition of the species present in the sample. Where possible, detailed phase analysis using microbeam techniques should be undertaken to establish the true composition for each phase. A complication that serves to decrease the agreement is that chemically based compositional analysis does not distinguish between crystalline and amorphous phase content, while the diffraction-based QPA usually measures only the crystalline phases. Generally, the composition of amorphous phases may not be known accurately and even highly crystalline material can contain amorphous components because of non-diffracting surface layers of the grains (Cline *et al.*, 2011).

An example demonstrating the level of agreement that can be achieved is that of the iron-ore certified reference material SX 11-14 from Dillinger Hütte (Fig. 3.9.22). The material is moderately complex and consists of nine distinct mineral species. The data were measured with Co $K\alpha$ radiation and analysed using Rietveld-based QPA in *TOPAS* (Bruker AXS, 2013). The phase abundances are converted to elemental and oxide compositions for comparison with the certified elemental analyses (Table 3.9.6). There is excellent agreement between the XRD results and the chemical analysis with bias values better than ±1 wt%.

3.9.10.3.6. *Phase-specific methods: diffraction SRMs, round-robin samples and synthetic mixtures*

In contrast to elemental compositional analysis, where standard reference materials (SRMs) are widespread, there are only a very limited number of SRMs available for diffraction-based QPA. Prominent examples are SRMs for the cement industry [NIST reference material clinker 8486 (Stutzman & Leigh, 2000) and ordinary Portland cement NIST SRM 2686] or ceramics materials (silicon nitride CRM BAM-S001) (Peplinski *et al.*, 2004). Similar to elemental standards, the certified values do not necessarily represent the true composition. Rather, they are published values that are typically averaged over the results from different independent methods, instruments and laboratories. Therefore, confidence limits of concentrations are provided that may be much larger than estimated standard deviations of concentrations within a single laboratory.

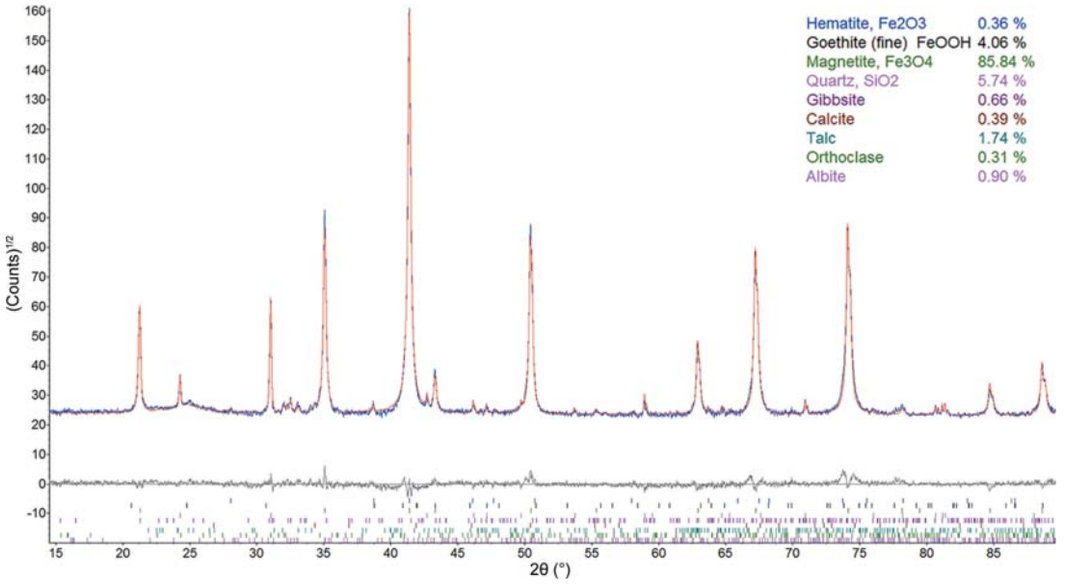


**Figure 3.9.22**
Output of Rietveld refinement and results of QPA for the iron-ore certified reference material SX 11-14 from Dillinger Hütte. The data were measured with Co $K\alpha$ radiation.

Finally, a number of inter-laboratory tests, or round robins, have been conducted on synthetic mixtures in order to set benchmarks for particular materials and/or the application of methods. Examples range from well ordered, high-symmetry phases discussed in earlier sections of this chapter (Madsen *et al.*, 2001; Scarlett *et al.*, 2002) to standard mixtures of geological material, granite and bauxites (Bish & Post, 1993), and technical products like artificial Portland cements (De la Torre & Aranda, 2003) where relative biases of 2–3% for the main phases and 5–10% for minor phases were found.

Very recently, the precision and accuracy of QPA for the analysis of Portland clinker and cement were determined for synthetic mixtures and commercial samples. The scatter of the results from the inter-laboratory comparison, and the fact that individual errors are much smaller than the standard deviations of all submitted results, points to the widespread presence of user-dependent systematic errors (Léon-Reina *et al.*, 2009).

One of the most challenging round robins is the Reynolds Cup (Ottner *et al.*, 2000; McCarty, 2002; Kleeberg, 2005; Omotoso *et al.*, 2006; Raven & Self, 2017), organized biannually since the year 2000 by the Clay Minerals Society. Synthetic mixtures representing typical sedimentary rock types are analysed and require a very high level of sample preparation and analytical skills because of the presence of a variety of clay minerals.

While most round robins have dealt with inorganic materials, one for pharmaceutical materials was organised by the International Centre for Diffraction Data (ICDD) together with the Pharmaceutical Powder XRD symposium series (PPXRD) (Fawcett *et al.*, 2010). A major outcome was the identification of operator errors in all steps of the analysis to be the largest source of error. This highlights the importance of reducing systematic errors for improving accuracy in QPA.

As a concluding remark, a variety of factors may influence the precision and accuracy of QPA. Nonetheless, better than 1 wt% agreement may be achieved for simple systems of well crystallized material. Moderately complex mixtures such as those routinely observed in cement plants and in the mining industry can be typically analysed at a 1 wt% level of accuracy provided that the analyst chooses the most appropriate sample-preparation, data-collection and analysis methodologies for the samples in question.

### 3.9.11. Summary

The value in using diffraction-based methods for the determination of phase abundance arises from the fact that the observed data are derived directly from the crystal structure of each phase. Knowledge of phase abundance is valuable in many fields including (i) mineral exploration, where the type and amount of major minerals serve as indicators for valuable minor minerals, (ii) mineral extraction, where the performance of the process line is governed by the mineralogy, not the commonly used elemental compositions, (iii) *in situ* studies, where the mechanism and kinetics of phase evolution resulting from the application of an external variable can be examined and (iv) the optimization of production conditions for advanced materials.

The methodology of QPA is fraught with difficulties, many of which are experimental or derive from sample-related issues. Hence, it is necessary to verify diffraction-based phase abundances against independent methods. This should include calculation of the expected sample element composition (using the QPA and an assumed or measured composition of each phase) and comparing these values with the measured element composition. In those circumstances where this is not possible, the QPA values should be regarded only as semi-quantitative. While such values may be useful for deriving trends within a particular system, they cannot be regarded as an absolute measure.

### References

Ahtee, M., Nurmela, M., Suortti, P. & Järvinen, M. (1989). *Correction for preferred orientation in Rietveld refinement. J. Appl. Cryst.* **22**, 261–268.
Alexander, L. E. & Klug, H. P. (1948). *Basic aspects of X-ray absorption in quantitative diffraction analysis of powder mixtures. Anal. Chem.* **20**, 886–889.
Ballirano, P. & Caminiti, R. (2001). *Rietveld refinements on laboratory energy dispersive X-ray diffraction (EDXD) data. J. Appl. Cryst.* **34**, 757–762.
Barnes, P., Colston, S., Craster, B., Hall, C., Jupe, A., Jacques, S., Cockcroft, J., Morgan, S., Johnson, M., O'Connor, D. & Bellotto, M.